The multi-objective optimization of the horizontal-axis marine current turbine based on NSGA-II algorithm

The multi-objective optimization of the horizontal-axis marine current turbine based on NSGA-II algorithm

G J Zhu[1,2], P C Guo[1,2], X Q Luo[1,2] and J J Feng[1,2]

[1] Institute of Water Resources and Hydro-Electric Engineering, Xi'an University of Technology, No.5 South Jinhua Road, Xi'an, 710048,China
[2] FINE Institute for Hydraulic Machinery, A-16F,Huaxing Times Plaza,No.478 Wensan Rd, Hangzhou, 310013,China

E-mail: guoyicheng@hotmail.com

Abstract. The present paper describes a hydrodynamic optimization technique for horizontal-axial marine current turbine. The pitch angle distribution is important to marine current turbine. In this paper, the pitch angle distribution curve is parameterized as four control points by Bezier curve method. The coordinates of the four control points are chosen as optimization variables, and the sample space are structured according to the Box-Behnken experimental design method (BBD). Then the power capture coefficient and axial thrust coefficient in design tip-speed ratio is obtained for all the elements in the sample space by CFD numerical simulation. The power capture coefficient and axial thrust are chosen as objective function, and quadratic polynomial regression equations are constructed to fit the relationship between the optimization variables and each objective function according to response surface model. With the obtained quadratic polynomial regression equations as performance prediction model, the marine current turbine is optimized using the NSGA-II multi-objective genetic algorithm, which finally offers an improved marine current turbine.

1. Introduction

The oceans contain a huge potential resource of energy and the ocean energy is non-polluting. In order to reduce current dependence of electrical energy on fossil and nuclear-fuelled power plant, the ocean-energy technologies should be improved to exploit more energy from oceans. The marine-current energy is one of the ocean energy which could be exploited and many devices are being studied for marine current energy conversion. The devices used for marine current energy convert contains two main types: horizontal axis and vertical axis. The device which most commonly used is horizontal axis. There are many corporations has carried out the research of the horizontal axis marine current turbine. Such as the Clean Current Power systems Incorporate in Canada, the Openhydro Corporation in Ireland, the Hammerfest Strom in Norway and so on [1]. All this corporations has carried out research works on horizontal axis marine current turbine (HAMCT). Additionally, A.S.Bahaj [2-5], who is the professor of University of Southampton, has engaging in the research of MCT for several years. The original rotor and experimental data in this paper are just from the work of Bahaj [2]. Based on NSGA-II and response surface methodology and in order to improve the power capture coefficient (C_P) and axial thrust coefficient (C_t), this paper regards the pitch angle distribution curve of original rotor as an object to optimize. During the optimization, the acquisition of rotor's C_P and C_T is according to CFD method.

2. Description of original rotor

The diameter of original rotor is 800mm. The rotor blades were developed from the profile shape of a NACA 63-8xx and a chord, thickness and pitch angle distribution as shown in Table 1[2]. The geometry model of rotor blades is shown in Fig. 1. The original rotor has been tested in the cavitation tunnel which has 5 meter length、2.4 meter breadth and 1.2 meter height [2].

Table 1. Particulars of rotor blades

r/R	Radius(mm)	*c/R*	Pitch angle distribution (deg)	*t/c* (%)
0.2	80	0.125	20.0	24.0
0.3	120	0.1156	14.5	20.7
0.4	160	0.1063	11.1	18.7
0.5	200	0.0969	8.9	17.6
0.6	240	0.0857	7.4	16.6
0.7	280	0.0781	6.5	15.6
0.8	320	0.0688	5.9	14.6
0.9	360	0.0594	5.4	13.6
1.0	400	0.0500	5.0	12.6

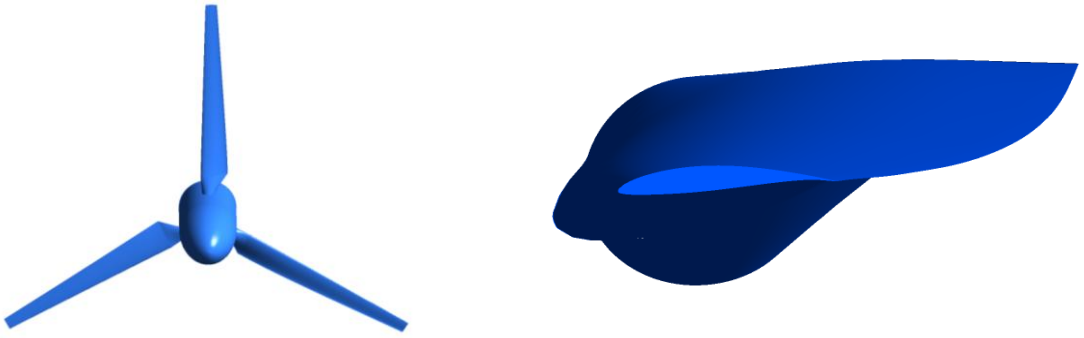

Figure 1. The geometry model of rotor blade

3. Parameterization of rotor blade

In order to optimize the rotor blade, first, it must be parameterized, and the second, the relationship between performance parameter and geometry parameter must be built. Because the rotor blades could be seem as constituted by many profile shapes of NACA 63-8xx which with fixed chord, thickness and pitch angle, so this paper keeps all airfoil section's chord and thickness invariant, and through controlling pitch angle distribution to define rotor blade's geometry. The pitch angle distribution could be expressed by pitch angle distribution curve. And according to three cubed Bézier curve parametric technology, the pitch angle distribution curve is controlled by four control points. Just as the Fig. 2 shows, the b_0、b_1、b_2 and b_3 are the control points of pitch angle distribution curve. The initial coordinates of b_0 to b_3 are reverse calculated based on original rotor blade's angle distribution curve. Δy_0、Δy_1、Δy_2 and Δy_3 are defined as the ordinate variation of b_0、b_1、b_2 and b_3, and kept their abscissa unchanged. So if the value of Δy_0、Δy_1、Δy_2 and Δy_3 are defined, the new position of b_0 to b_3 could be determined. Knowing the exact position of the four points (b_0、b_1、b_2、b_3), the pitch angle distribution curve is reconstructed based on fitting formula of Bézier curve. The formula of Bézier curve is:

$$\vec{p}(t)=\sum_{i=0}^{n}\vec{b}_i B_{i,n}(t), 0\le t\le 1 \qquad (1)$$

where $\vec{p}(t)$ is the vector of data point, $\vec{b}_i$ (i=0,1,2,3) is the vector of control point, and $B_{i,n}(t)$ is the Bernstein basic function. For the sake of keeping rotor blade has a smooth and reasonable geometry, the parameter space of variables are showed in Table 2.

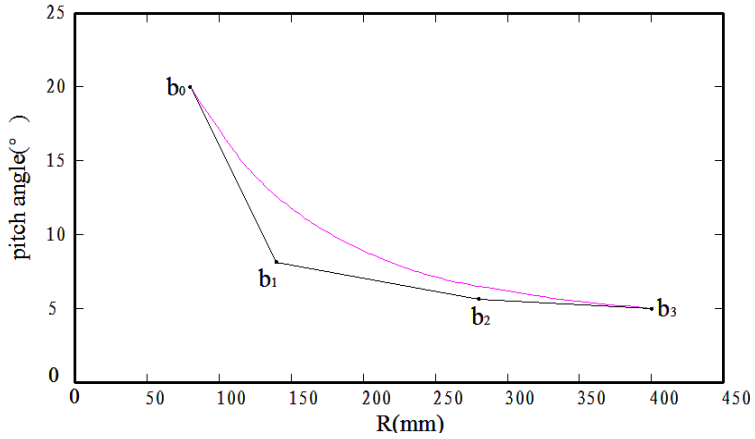

Figure 2. The control points of pitch angle distribution curve

Table 2. Parameter space for the moving points b_0 to b_3.

Point	Parameter	Minimum (°)	Maximum (°)
b_0	Δy_0	-3	4
b_1	Δy_1	-3	5
b_2	Δy_2	0	3
b_3	Δy_3	-2	0

4. Numerical flow simulations

The flow region is divided into two parts. One is the rotor domain, and the other is the stay domain. The stay domain is a rectangle which has 8 meter length、2.4 meter breadth and 1.2 meter height and the rotor domain which contain runner is a circle which diameter is 0.84 meter. The distance between runner and the flow region inlet is two times of the runner's diameter and the distance between runner and outlet is eight times of the runner's diameter. The rotor domain and stay domain are discreet by structure mesh. The nodes of rotor domain are about 2 million, and the nodes of stay domain are 1.9 million. The mesh is shown in Fig. 3. All flow simulations presented in this work rely on the industrial software ANSYS-CFX. The steady-state Reynolds-Averaged Navier-Stokes equations are solved using SIMPLEC algorithm for pressure-velocity coupling. And the turbulence model used in CFD evaluation is SST $k-\omega$ model. The optimization is carried out in design TSR condition, so the flow condition is set to be in the design TSR, with the inlet velocity of 1.73m/s. The static pressure of 0 Pa is defined as a boundary condition at the outlet.

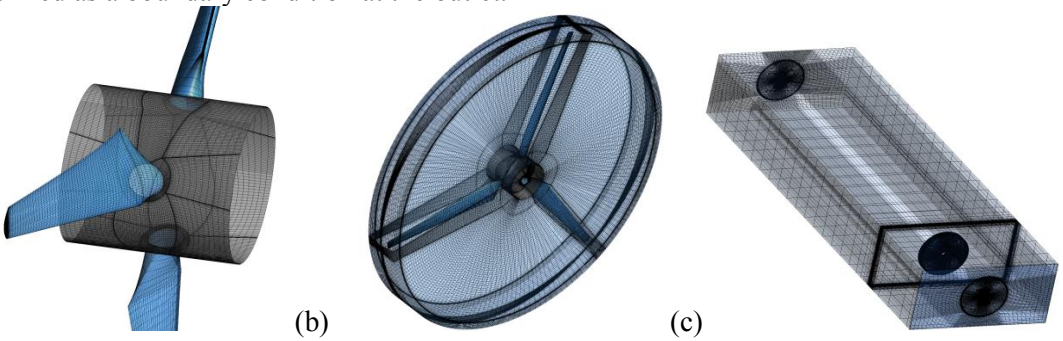

Figure 3. Mesh of the flow region (a) Blade (b) Rotor Domain (c) Stay Domain

The TSR, power (C_P) and thrust (C_t) coefficients were dimensioned as the same as A.S.Bahaj's paper [2]. As shown in Fig. 4, the accuracy of CFD simulation is validated by comparison the published experimental data with CFD result about original rotor blade at four TSR flow condition.

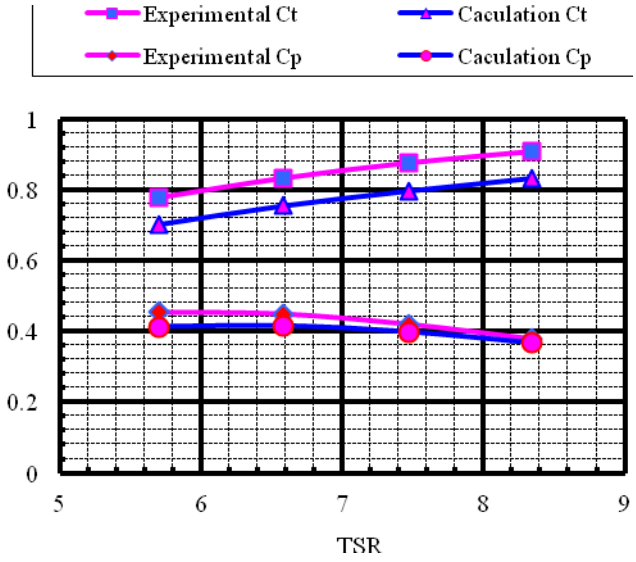

Figure 4. The comparison of experiment to CFD about power coefficients and thrust coefficients

5. Optimization methodology

Optimization methods attempt to establish a relationship between design variables and objective functions. In the present paper, the free design variables considered for the optimization are Δy_0、Δy_1、Δy_2 and Δy_3, which are the ordinate variation of b_0、b_1、b_2 and b_3. The objective functions are the power (C_P) and thrust (C_t) coefficients, which obtain according to CFD calculation. The response surface model has been used to fit the relationship between design variables and objective functions. The sample space is structured according to the BBD experimental design method. The factor's level is three. The code of low level and high level are separately set to -1 and 1, and the code of middle level is set to 0. So the value of each factor level is shown in Table 3.

Table 3. The value of each factor level

Design Variable	Low level		Middle level		High level	
	Code value	Real value	Code value	Real value	Code value	Real value
Δy_0	-1	-3	0	0.5	1	4
Δy_1	-1	-3	0	1	1	5
Δy_2	-1	0	0	1.5	1	3
Δy_3	-1	-2	0	-1	1	0

Based on the BBD experimental design method, the total experiment times are 29. And the arrangement of experiment design is shown in Table 4.

Table 4. Arrangement of experiment

Variable	Arrangement of experiment base on code value																												
Δy_0	0	-1	0	0	0	0	0	0	0	0	-1	-1	0	0	-1	0	1	-1	1	0	0	0	1	0	0	-1	1	1	1
Δy_1	-1	0	1	0	-1	1	0	0	0	0	0	-1	-1	0	0	-1	0	0	0	0	1	0	0	1	0	1	0	-1	1
Δy_2	-1	0	0	0	0	0	-1	0	-1	0	1	0	1	1	0	0	0	-1	1	0	-1	0	0	1	1	0	-1	0	0
Δy_3	0	-1	1	0	1	-1	1	0	-1	0	0	0	0	-1	1	-1	1	0	0	0	0	0	-1	0	1	0	0	0	0

At each experimental, the objective function are obtain by CFD calculation, and their value are shown in Fig. 5.

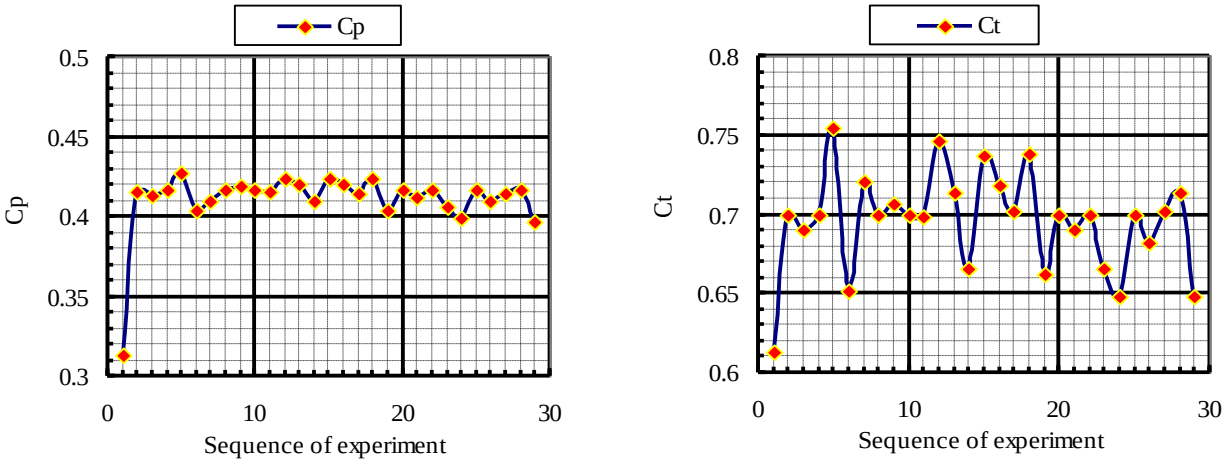

Figure 5. The distribution of objective function in experiment

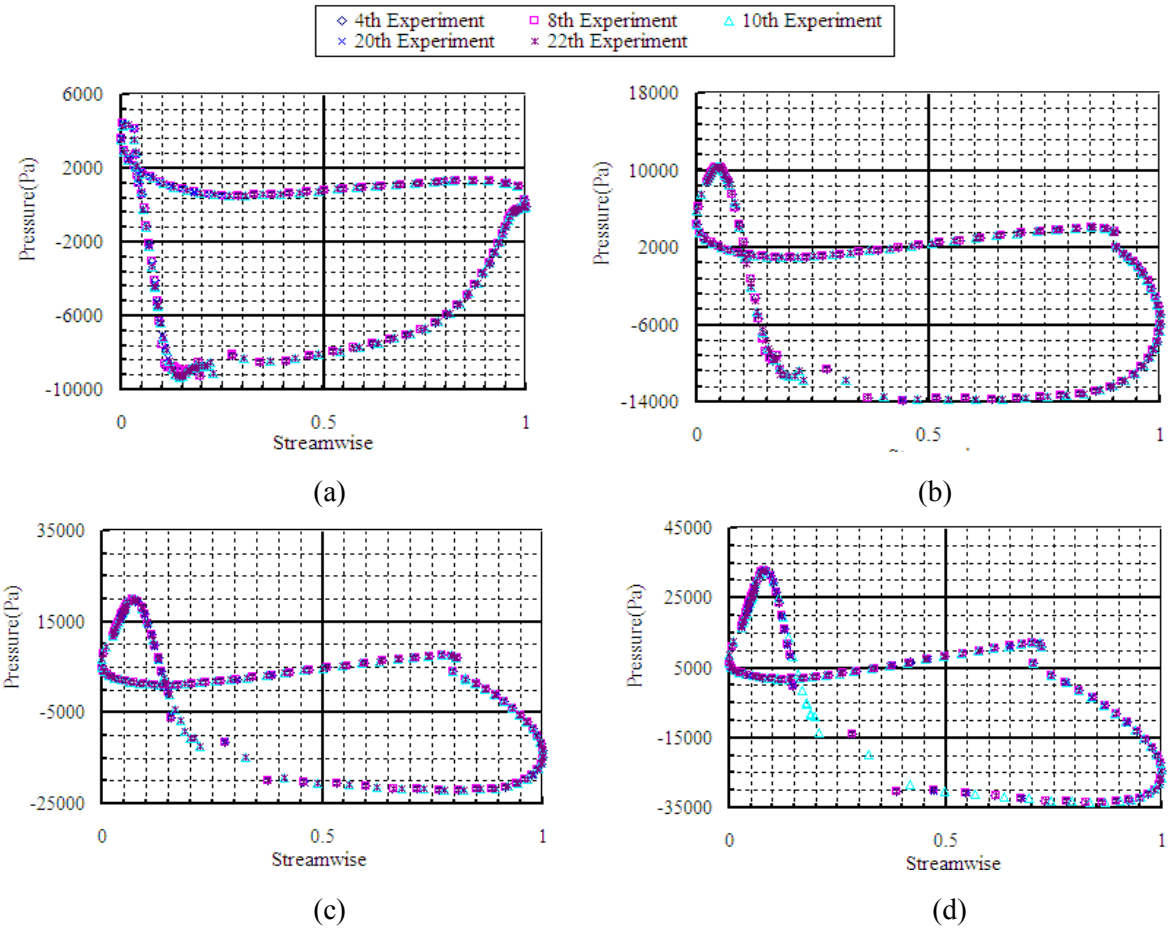

Figure 6. The pressure distribution at different span of blade in five times experiments about central point (a) 0.1 Span (b) 0.3 Span (c) 0.5 Span (d) 0.7 Span

According to the BBD experiment design method, the experiment about central point of sample space must be repeated for five times to ensure the experiment has enough precision. As shown in Fig. 6, in five times experiments of central point, the pressure distribution of blade is almost the same. It means that the design of experiment meets the requirement of consistency.

Based on the experiment result, the response surface model is established as follows:

$$\begin{aligned} C_P = {} & 0.39822 + A_1 * \Delta y_0 + A_2 * \Delta y_1 + A_3 * \Delta y_2 + A_4 * \Delta y_3 \\ & + A_5 * \Delta y_0 * \Delta y_1 + A_6 * \Delta y_0 * \Delta y_2 + A_7 * \Delta y_0 * \Delta y_3 + A_8 * \Delta y_1 * \Delta y_2 + A_9 * \Delta y_1 * \Delta y_3 + A_{10} * \Delta y_2 * \Delta y_3 \\ & + A_{11} * \Delta y_0^{\,2} + A_{12} * \Delta y_1^{\,2} + A_{13} * \Delta y_2^{\,2} + A_{14} * \Delta y_3^{\,2} \end{aligned} \quad (2)$$

$$\begin{aligned} C_t = {} & 0.39822 + B_1 * \Delta y_0 + B_2 * \Delta y_1 + B_3 * \Delta y_2 + B_4 * \Delta y_3 \\ & + B_5 * \Delta y_0 * \Delta y_1 + B_6 * \Delta y_0 * \Delta y_2 + B_7 * \Delta y_0 * \Delta y_3 + B_8 * \Delta y_1 * \Delta y_2 + B_9 * \Delta y_1 * \Delta y_3 + B_{10} * \Delta y_2 * \Delta y_3 \\ & + B_{11} * \Delta y_0^{\,2} + B_{12} * \Delta y_1^{\,2} + B_{13} * \Delta y_2^{\,2} + B_{14} * \Delta y_3^{\,2} \end{aligned} \quad (3)$$

The value of $A_n, (n = 1, 2, \cdots, 14)$ and $B_n, (n = 1, 2, \cdots, 14)$ is shown in Table 5.

Table 5. The value of A_n and B_n

Variable	Value	Variable	Value
A_1	-1.36735E-003	B_1	-5.21259E-003
A_2	9.05060E-003	B_2	4.95536E-003
A_3	0.020270	B_3	0.014417
A_4	0.011125	B_4	2.17262E-003
A_5	-1.42857E-004	B_5	-3.57143E-005
A_6	-9.52381E-005	B_6	5.20417E-018
A_7	4.58463E-018	B_7	7.14286E-005
A_8	-5.00000E-003	B_8	-5.91667E-003
A_9	-1.25000E-004	B_9	-1.25000E-004
A_{10}	-2.66667E-003	B_{10}	-3.16667E-003
A_{11}	2.24490E-004	B_{11}	3.91156E-004
A_{12}	-6.56250E-004	B_{12}	-6.77083E-004
A_{13}	-4.66667E-003	B_{13}	-5.42593E-003
A_{14}	4.75000E-003	B_{14}	6.91667E-003

Then based on the response surface model, the relationship between objective function and geometry parameter is fitted. So the geometry parameter of rotor blade can be optimized by NSGA-II. The NSGA-II is a multi objective GA which has been used for a long time in optimal region. It has been verified that with high efficiency in searching pareto solution. In this paper, the population size of NSGA-II is set to 24, and the number of generations is set to 25. The crossover probability is set to 0.7, and the mutation probability is set to 0.8. The optimization results of objective function are shown in Fig. 7.

As shown in Fig. 7, the distribution of pareto solutions in this optimal is even. According to compare the pareto solution, a solution which with best comprehensive performance has been selected. And in order to affirm the optimization is effective, the performance of selected optimal rotor blade in design TSR is evaluated by CFD. The number and topology of structure grid which used for evaluate the performance of initial blade and optimization is the same. The comparison of optimal rotor and initial rotor about variable and objective function which obtained by CFD is shown in table 6. And the comparison of pitch angle distribution curve is shown in Fig. 8. The comparison of geometry between optimal blade and initial blade is shown in Fig. 9. From the table 6, we can see that the power capture coefficient of optimal rotor blade is raised, and the axial thrust coefficient of optimal rotor blade is decreased, which means the optimal rotor with better efficiency and less thrust in working.

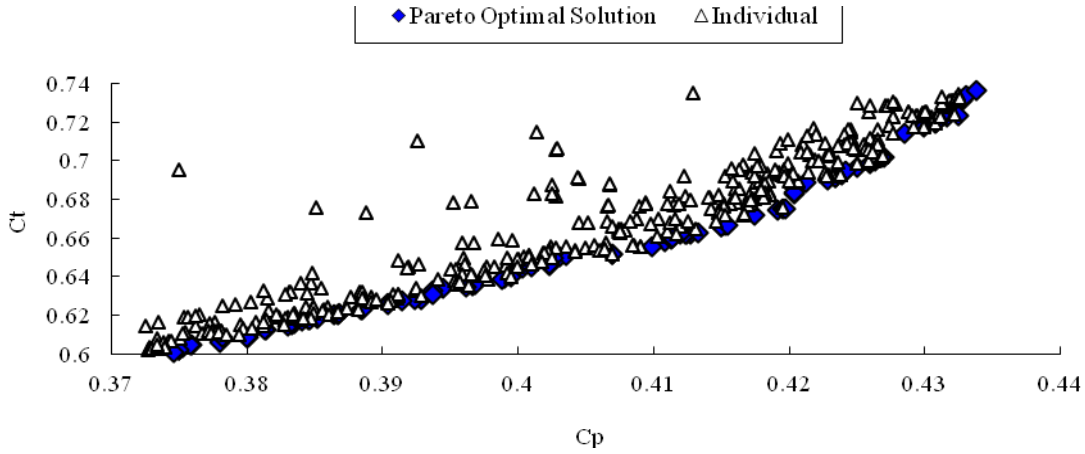

Figure 7. Optimization result of C_p and C_t

Table 6. The variable value of the selected optimal solution

Variable name	Δy_0	Δy_1	Δy_2	Δy_3	C_P	C_t
Initial value	0	0	0	0	0.413	0.702
Optimal value	0.936	-2.385	2.954	-0.352	0.417	0.682

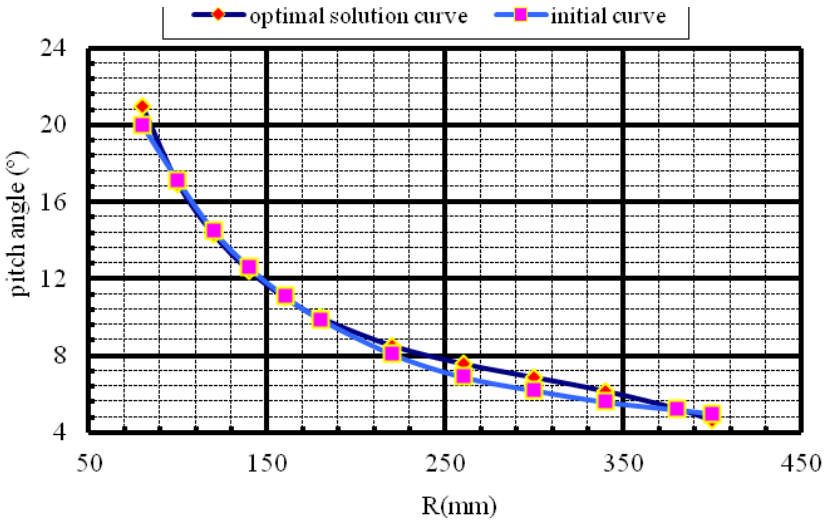

Figure 8. The comparison of pitch angle distribution curve between optimal solution and initial

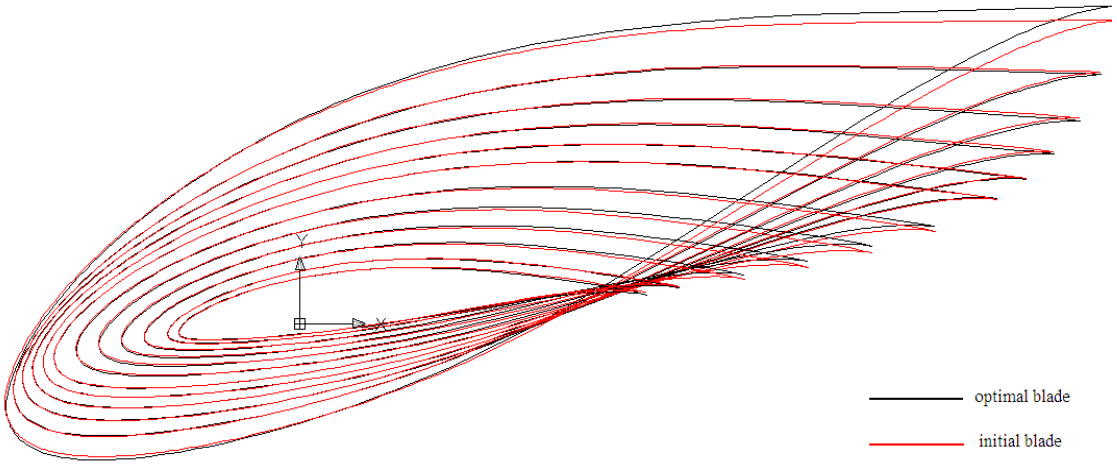

Figure 9. The comparison of geometry between optimal rotor blade and initial blade

6. Conclusions

An approach for optimization of power capture coefficient and axial thrust coefficient of marine current turbine was presented in this paper. According to the Bézier curve parametric technology, the geometry of rotor blade is established by four variables. The power capture coefficient (C_p) and axial thrust coefficient (C_t) are selected as objectives. And the relationship between geometrical variables and objective function is fitted by BBD experiment design method and response surface method. Then the two objectives have been optimized in a concurrent manner. The optimization relies on NSGA-II Algorithms, and the two objectives of all individuals are evaluated by CFD.

This optimization procedure is able to identify a considerably better configuration than the initial rotor. A relative increase of the power capture coefficient is 0.4%. In the mean while, the axial thrust coefficient didn't go worst.

Acknowledgments

The Research was supported by the National Natural Science Foundation of China (50979091), the Specialized Research Fund for the Doctoral Program of Higher Education of China(20096118110012), the Special Fund of State Key Laboratory of Eco-Hydraulic Engineering in Shaanxi Province, the Natural Science Basic Research Plan in Shaanxi Province of China(2012JM7005), the Scientific Research Program Funded by Shaanxi Provincial Education Department(2010JK735).

Nomenclature

R	blade tip radius (mm)
t	section thickness (mm)
c	blade chord (mm)
TSR	tip speed ratio

References

[1] Liu H W, Ma S, Li W, Gu H G, Lin Y G and Sun X J 2011 *Renewable and Sustainable Energy Rev.* **15** 1141-1146
[2] Batten W M J, Bahaj A S, Molland A F and Chaplin J R 2007 *Ocean Engineering* **34** 1013-1020
[3] Bahaj A S, Molland A F, Chaplin J R and Batten W M J 2007 *Renewable Energy* **32** 407-426
[4] Batten W M J, Bahaj A S, Molland A F and Chaplin J R 2008 *Renewable Energy* **33** 1085-1096
[5] Bahaj A S, Batten W M J and McCann G 2007 *Renewable Energy* **32** 2479-2490
[6] Stephen R T, Alexander B P, Joe B and Rachel N L 2011 *Ocean Engineering* **38** 1300-1307